

Cross section measurements on zirconium isotopes for ~14 MeV neutrons and their theoretical calculations of excitation functions*

Yong Li(李勇)¹ Yueli Song(宋月丽)¹ Fengqun Zhou(周丰群)^{1,1)} Xinyi Chang(畅心怡)^{1,2}
Xiaopeng Zhang(张晓朋)¹ Mingli Tian(田明丽)¹ Shuqing Yuan(袁书卿)¹

¹School of Electrical and Mechanical Engineering, Pingdingshan University, Pingdingshan 467000, China

²School of Physics and Engineering, Zhengzhou university, Zhengzhou 450001, China

Abstract: The cross sections for the $^{94}\text{Zr}(n,d^*)^{93\text{m}+g}\text{Y}$, $^{96}\text{Zr}(n,\gamma)^{97}\text{Zr}$, $^{96}\text{Zr}(n,2n)^{95}\text{Zr}$, $^{90}\text{Zr}(n,\alpha)^{87\text{m}}\text{Sr}$, $^{94}\text{Zr}(n,\alpha)^{91}\text{Sr}$, $^{90}\text{Zr}(n,p)^{90\text{m}}\text{Y}$, $^{92}\text{Zr}(n,p)^{92}\text{Y}$, and $^{94}\text{Zr}(n,p)^{94}\text{Y}$ reactions have been measured in the neutron energy range of 13.5-14.8 MeV by means of the activation technique. The neutrons were produced via the D-T reaction. A high-purity germanium detector with high energy resolution was used to measure the induced γ activities. In combination with the nuclear reaction theoretical models, the excitation curves of the above-mentioned eight nuclear reactions within the incident neutron energy range from the threshold to 20 MeV were obtained by adopting the nuclear theoretical model program system Talys-1.9. The resulting experimental cross sections were analyzed and compared with the experimental data from published studies. Calculations were performed using Talys-1.9 and are in agreement with our experimental results, previous experimental values, as well as results of the theoretical excitation curves at the corresponding energies. The theoretical excitation curves generally match the experimental data well.

Keywords: zirconium isotopes, cross section, 14 MeV neutrons, activation methods, theoretical calculations

DOI: 10.1088/1674-1137/abb4d3

1 Introduction

Zirconium metal and its alloys are widely used in national defense, aerospace, atomic energy, and other fields owing to their excellent physical and chemical properties. Accurate nuclear reaction cross sections on zirconium isotopes around 14 MeV neutrons are crucial for the development of nuclear weapons, development and utilization of nuclear energy, application of nuclear technology, etc. Therefore, these cross sections of $(n,2n)$, (n,α) , (n,p) , (n,d) , and (n,γ) reactions on zirconium isotopes around 14 MeV neutrons have been studied by numerous researchers worldwide and can be found in the experimental nuclear reaction data (EXFOR) library [1]. However, the cross section of the $^{94}\text{Zr}(n,d^*)^{93\text{m}+g}\text{Y}$ [$d^*=d+(n+p)$, similarly hereinafter] reaction has been measured by only two groups at single neutron energies of 14.7 MeV or 14.1 MeV, and there is a large difference between the two values obtained, which are 2.43 ± 0.21 mb [2] and 0.8 ± 0.1 mb [3], respectively. For the $^{96}\text{Zr}(n,\gamma)^{97}\text{Zr}$ reaction, the cross section has been measured by more than 20 groups

[1]; however, three of them were induced by neutrons through the D-T reaction [4-6], and there are significant differences in those data, the maximum difference between them being more than a factor of 30. Thus, it is necessary to measure them again and provide their excitation functions. In this work, the cross sections of the $^{94}\text{Zr}(n,d^*)^{93\text{m}+g}\text{Y}$ and $^{96}\text{Zr}(n,\gamma)^{97}\text{Zr}$ reactions have been measured in the neutron energy range of 13.5-14.8 MeV via the activation technique. At the same time, combined with the theoretical models of nuclear reactions, the computations of the excitation functions of the above-mentioned two nuclear reactions were conducted by adopting the nuclear theoretical model program system Talys-1.9 [7]. Their excitation curves were acquired in the neutron energy range from the threshold to 20 MeV. In addition, the cross sections of the $^{96}\text{Zr}(n,2n)^{95}\text{Zr}$, $^{90}\text{Zr}(n,\alpha)^{87\text{m}}\text{Sr}$, $^{94}\text{Zr}(n,\alpha)^{91}\text{Sr}$, $^{90}\text{Zr}(n,p)^{90\text{m}}\text{Y}$, $^{92}\text{Zr}(n,p)^{92}\text{Y}$, and $^{94}\text{Zr}(n,p)^{94}\text{Y}$ reactions of ~14 MeV neutrons were measured, and their excitation curves in the neutron energy range from the threshold to 20 MeV were acquired. The cross sections obtained are compared with earlier experiments by other

Received 10 July 2020, Published online 7 October 2020

* Supported by the National Natural Science Foundation of China (11575090)

1) E-mail: zfq@pdsu.edu.cn

©2020 Chinese Physical Society and the Institute of High Energy Physics of the Chinese Academy of Sciences and the Institute of Modern Physics of the Chinese Academy of Sciences and IOP Publishing Ltd

researchers and with the theoretical results obtained by Talys-1.9.

2 Experimental

Natural zirconium foils (purity: 99.99%, thickness: 3.04-3.09 mm) were formed into round disks with a diameter of 20 mm. Four such round disks were prepared. Niobium monitor foils (purity: 99.95%, thickness: 0.62 mm) of the same diameter as the zirconium sample were subsequently fixed at the front and back of each zirconium sample, which was wrapped in a cadmium foil (purity: 99.95%, thickness: 1 mm) to reduce the influence of the $^{94}\text{Zr}(n,\gamma)^{95}\text{Zr}$ reaction induced by low-energy neutrons on $^{96}\text{Zr}(n,2n)^{95}\text{Zr}$ reactions.

The samples were irradiated at the K-400 Neutron Generator at China Academy of Engineering Physics (CAEP) for 6.2-7.5 h. Neutrons around 14 MeV with an yield of about $(4-5)\times 10^{10} \text{ n}\cdot\text{s}^{-1}$ were generated via the D-T reaction with a deuteron beam energy of 255 keV and a beam current of 300-400 μA . The thickness of the solid tritium-titanium (T-Ti) target applied to the generator was $2.19 \text{ mg}\cdot\text{cm}^{-2}$. For the irradiation of the samples, an Au-Si surface barrier detector was used at 135° accompanying α particle tube to correct small variations in neutron flux. The samples were placed at 0° - 135° angles relative to the direction of the deuteron beam, and the distances from the center of the T-Ti target were approximately 40-50 mm (as shown in Fig. 1). The neutron energies in the measurements depend on the averages of cross section ratios for the $^{90}\text{Zr}(n,2n)^{89\text{m}+\text{g}}\text{Zr}$ and $^{93}\text{Nb}(n,2n)^{92\text{m}}\text{Nb}$ reactions [8].

The γ -ray activities of $^{93\text{m}+\text{g}}\text{Y}$, ^{97}Zr , ^{95}Zr , $^{87\text{m}}\text{Sr}$, ^{91}Sr , $^{90\text{m}}\text{Y}$, ^{92}Y , ^{94}Y , and $^{92\text{m}}\text{Nb}$ were determined by a well-calibrated GEM-60P coaxial high-purity germanium ORTEC detector made in the USA (crystal diameter: 70.1 mm, crystal length: 72.3 mm) with a relative efficiency of 68% and an energy resolution of 1.69 keV at 1.332 MeV.

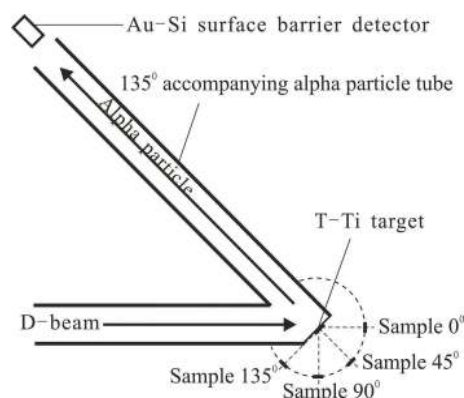


Fig. 1. Schematic diagram of neutron flux variation monitoring and sample placement.

The efficiency of the detector was calibrated in advance using a series of standard γ sources.

Decay characteristics of the product nuclides and the natural abundance of target isotopes under investigation are summarized in Table 1 [9]. The natural abundance of ^{93}Nb is adopted from Ref. [10].

3 Data analysis

The measured cross sections were calculated by the formula provided by Xiangzhong Kong *et al.* [11].

The experimental cross sections of the $^{94}\text{Zr}(n,d^*)^{93\text{m}+\text{g}}\text{Y}$, $^{96}\text{Zr}(n,\gamma)^{97}\text{Zr}$, $^{96}\text{Zr}(n,2n)^{95}\text{Zr}$, $^{90}\text{Zr}(n,\alpha)^{87\text{m}}\text{Sr}$, $^{94}\text{Zr}(n,\alpha)^{91}\text{Sr}$, $^{90}\text{Zr}(n,p)^{90\text{m}}\text{Y}$, $^{92}\text{Zr}(n,p)^{92}\text{Y}$, and $^{94}\text{Zr}(n,p)^{94}\text{Y}$ reactions were acquired. The monitor reaction was the $^{93}\text{Nb}(n,2n)^{92\text{m}}\text{Nb}$ reaction, whose cross sections are 457.9 ± 6.8 , 459.8 ± 6.8 , 459.8 ± 6.8 , and 459.7 ± 5.0 mb at the neutron energies of 13.5, 14.1, 14.4, and 14.8 MeV, respectively [12]. The measured cross sections are listed in Table 2 and charted in Figs. 2-9. The cross sections of the $^{94}\text{Zr}(n,d^*)^{93\text{m}+\text{g}}\text{Y}$, $^{96}\text{Zr}(n,\gamma)^{97}\text{Zr}$, $^{96}\text{Zr}(n,2n)^{95}\text{Zr}$, $^{90}\text{Zr}(n,\alpha)^{87\text{m}}\text{Sr}$, $^{94}\text{Zr}(n,\alpha)^{91}\text{Sr}$, $^{90}\text{Zr}(n,p)^{90\text{m}}\text{Y}$, $^{92}\text{Zr}(n,p)^{92}\text{Y}$, and $^{94}\text{Zr}(n,p)^{94}\text{Y}$ reactions around 14 MeV neutrons have

Table 1. Reactions and associated decay data of product nuclides.

reaction	abundance of target isotope (%)	product nuclides	$T_{1/2}$	E_γ/keV	I_γ (%)
$^{94}\text{Zr}(n,d^*)$	17.38	$^{93\text{m}+\text{g}}\text{Y}$	10.18 h	266.9	7.4
$^{96}\text{Zr}(n,\gamma)$	2.8	^{97}Zr	16.749 h	743.36	93.09
$^{96}\text{Zr}(n,2n)$	2.8	^{95}Zr	64.032 d	756.725	54.38
$^{90}\text{Zr}(n,\alpha)$	51.45	$^{87\text{m}}\text{Sr}$	2.815 h	388.531	82.19
$^{94}\text{Zr}(n,\alpha)$	17.38	^{91}Sr	9.65 h	1024.3	33.5
$^{90}\text{Zr}(n,p)$	51.45	$^{90\text{m}}\text{Y}$	3.19 h	479.51	90.74
$^{92}\text{Zr}(n,p)$	17.15	^{92}Y	3.54 h	934.47	13.9
$^{94}\text{Zr}(n,p)$	17.38	^{94}Y	18.7 m	918.74	56
$^{93}\text{Nb}(n,2n)$	100	$^{92\text{m}}\text{Nb}$	10.15 d	934.44	99.15

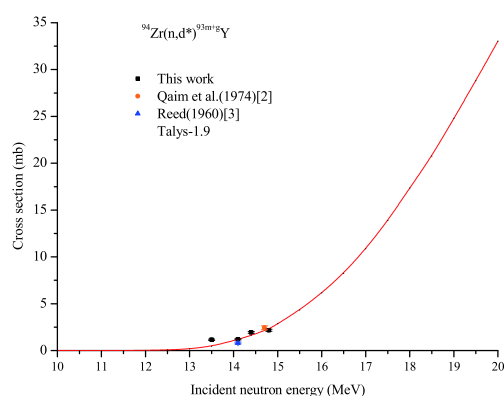
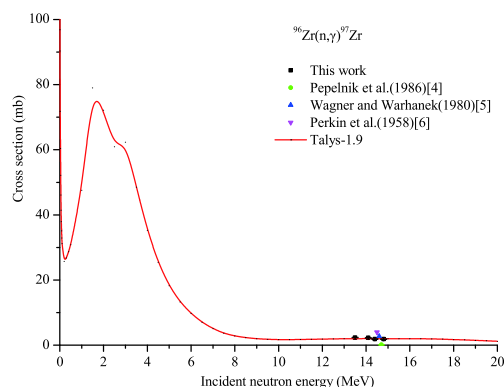
Table 2. Summary of cross section measurements.

reaction	the measured cross sections (in mb) at various neutron energies (in MeV) literature values E_n /MeV, σ /mb			
	$E_n=13.5\pm 0.3$	$E_n=14.1\pm 0.2$	$E_n=14.4\pm 0.3$	$E_n=14.8\pm 0.2$
$^{94}\text{Zr}(n,d^*)^{93m+g}\text{Y}$	1.15±0.06	1.19±0.06	1.93±0.09	2.17±0.10
$^{96}\text{Zr}(n,\gamma)^{97}\text{Zr}$	2.33±0.10	2.24±0.09	1.85±0.09	1.84±0.08
$^{96}\text{Zr}(n,2n)^{95}\text{Zr}$	1502±63	1520±66	1521±68	1577±70
$^{90}\text{Zr}(n,\alpha)^{87m}\text{Sr}$	2.9±0.2	3.1±0.2	3.6±0.2	3.6±0.2
$^{94}\text{Zr}(n,\alpha)^{91}\text{Sr}$	3.86±0.16	4.10±0.18	4.77±0.20	5.09±0.22
$^{90}\text{Zr}(n,p)^{90m}\text{Y}$	9.8±0.4	10.1±0.5	11.4±0.5	11.1±0.5
$^{92}\text{Zr}(n,p)^{92}\text{Y}$	17.2±0.7	17.8±0.8	21.4±0.9	20.2±0.9
$^{94}\text{Zr}(n,p)^{94}\text{Y}$	5.2±0.3	6.5±0.3		7.3±0.4

been measured by 2, 4, 12, 22, 20, 24, 21, 23 groups, respectively [1]. Previously obtained experimental cross sections around 14 MeV neutrons for the $^{94}\text{Zr}(n,d^*)^{93m+g}\text{Y}$ and $^{96}\text{Zr}(n,\gamma)^{97}\text{Zr}$ reactions [2-6] are also charted in Figs. 2-3 for comparison. For the remainder, previous measurements [13-24], whose results were published after 1990, are charted in Figs. 4-9 for comparison.

Theoretical calculations of excitation functions of the $^{94}\text{Zr}(n,d^*)^{93m+g}\text{Y}$, $^{96}\text{Zr}(n,\gamma)^{97}\text{Zr}$, $^{96}\text{Zr}(n,2n)^{95}\text{Zr}$, $^{90}\text{Zr}(n,\alpha)^{87m}\text{Sr}$, $^{94}\text{Zr}(n,\alpha)^{91}\text{Sr}$, $^{90}\text{Zr}(n,p)^{90m}\text{Y}$, $^{92}\text{Zr}(n,p)^{92}\text{Y}$, and $^{94}\text{Zr}(n,p)^{94}\text{Y}$ reactions were performed using the nuclear theoretical model program system Talys-1.9, fully described in the Talys-1.9 manual [7]. Their excitation curves were obtained within the incident neutron energy range from the threshold to 20 MeV, as shown in Figs. 2-9 for comparison. Different parameters in the theoretical model program system Talys-1.9 were set according to our experimental cross sections and the results in previously published works [2-6, 13-24] for different nuclear reactions. For example, the optical model potential (OMP) parameter r_V was set for the $^{96}\text{Zr}(n,\gamma)^{97}\text{Zr}$, $^{96}\text{Zr}(n,2n)^{95}\text{Zr}$, and $^{90}\text{Zr}(n,\alpha)^{87m}\text{Sr}$ reactions, the OMP parameter r_V and a_V were set for the $^{94}\text{Zr}(n,d^*)^{93m+g}\text{Y}$, $^{94}\text{Zr}(n,\alpha)^{91}\text{Sr}$, and $^{92}\text{Zr}(n,p)^{92}\text{Y}$ reactions, the OMP parameter r_V , a_V and the level density parameter at the neutron separation energy were set for the $^{94}\text{Zr}(n,p)^{94}\text{Y}$ reaction, the OMP parameter r_V , a_V , model for level densities and the overall constant for the matrix element or the optical model strength in the exciton model were set for the $^{90}\text{Zr}(n,p)^{90m}\text{Y}$ reaction.

Talys-1.9 (latest version of the TALYS code) is a computer code used for the analysis and prediction of nuclear reactions based on physics models and parameterizations [7]. It is a versatile tool for the analyses of basic microscopic scientific experiments or generation of nuclear data for applications. It can simulate nuclear reactions involving neutrons, photons, protons, deuterons, tritons, ^3He , and alpha-particles in the 1 keV-200 MeV en-


 Fig. 2. (color online) Cross section of $^{94}\text{Zr}(n,d^*)^{93m+g}\text{Y}$ reaction.

 Fig. 3. (color online) Cross section of $^{96}\text{Zr}(n,\gamma)^{97}\text{Zr}$ reaction.

ergy range and for target nuclides of mass number range ($12 < A < 339$) [7]. Therefore, the TALYS code has been widely used in relevant research by most scientists [25-28].

Two or more reactions may produce the same product nucleus due to the use of natural zirconium foils in this work. These include the $^{96}\text{Zr}(n,2n)^{95}\text{Zr}$ and $^{94}\text{Zr}(n,\gamma)^{95}\text{Zr}$ reactions, the $^{90}\text{Zr}(n,\alpha)^{87m}\text{Sr}$ and $^{91}\text{Zr}(n,\alpha)^{87m}\text{Sr}$ reactions, the $^{90}\text{Zr}(n,p)^{90m}\text{Y}$, $^{91}\text{Zr}(n,d^*)^{90m}\text{Y}$ and $^{92}\text{Zr}(n,t)^{90m}\text{Y}$ reactions, the $^{92}\text{Zr}(n,p)^{92}\text{Y}$ and $^{94}\text{Zr}(n,t)^{92}\text{Y}$ reactions, and

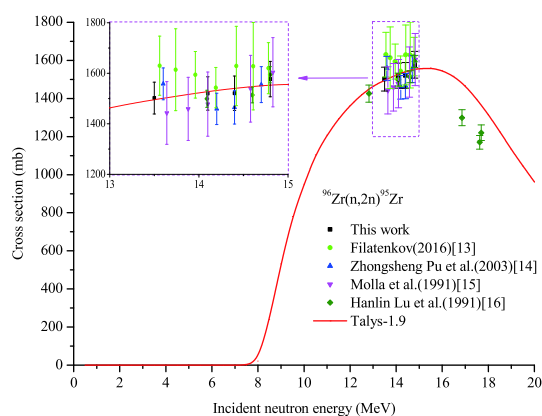


Fig. 4. (color online) Cross section of $^{96}\text{Zr}(n,2n)^{95}\text{Zr}$ reaction.

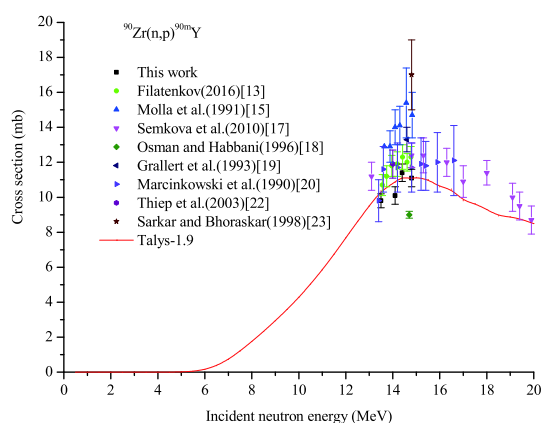


Fig. 7. (color online) Cross section of $^{90}\text{Zr}(n,p)^{90m}\text{Y}$ reaction.

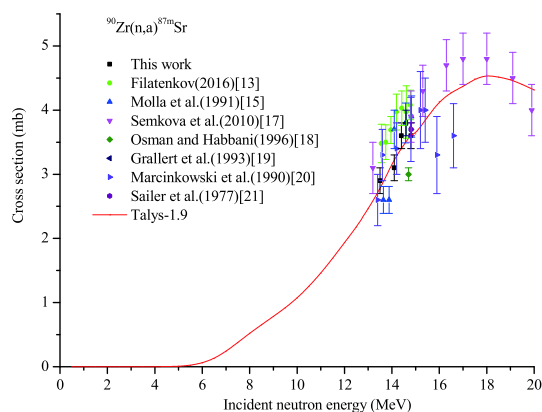


Fig. 5. (color online) Cross section of $^{90}\text{Zr}(n,\alpha)^{87m}\text{Sr}$ reaction.

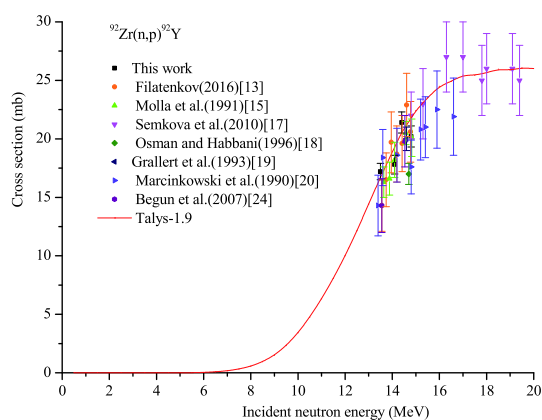


Fig. 8. (color online) Cross section of $^{92}\text{Zr}(n,p)^{92}\text{Y}$ reaction.

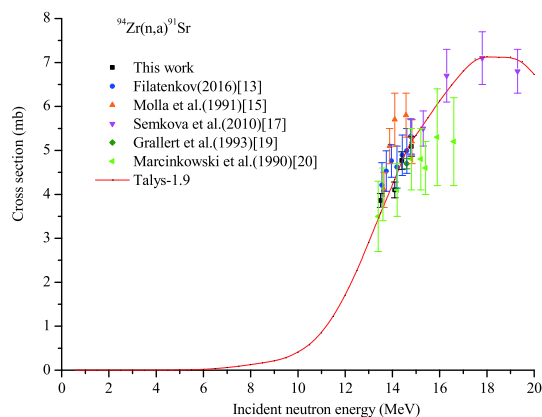


Fig. 6. (color online) Cross section of $^{94}\text{Zr}(n,\alpha)^{91}\text{Sr}$ reaction.

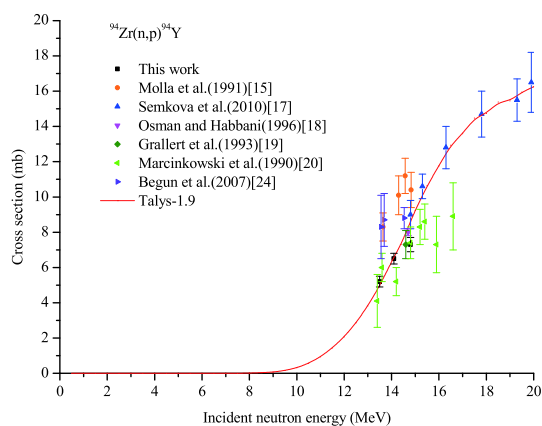


Fig. 9. (color online) Cross section of $^{94}\text{Zr}(n,p)^{94}\text{Y}$ reaction.

the $^{94}\text{Zr}(n,p)^{94}\text{Y}$ and $^{96}\text{Zr}(n,t)^{94}\text{Y}$ reactions. Thus, the cross sections obtained for the $^{96}\text{Zr}(n,2n)^{95}\text{Zr}$ reaction include the contribution from the $^{94}\text{Zr}(n,\gamma)^{95}\text{Zr}$ reaction, which can be neglected, as it has a very small cross section (μb) around the neutron energy of 14 MeV. The cross sections obtained for the $^{90}\text{Zr}(n,\alpha)^{87m}\text{Sr}$ reaction include the contribution of the $^{91}\text{Zr}(n,n'\alpha)^{87m}\text{Sr}$ reaction, which can be neglected as it has a very small cross section (μb). The cross

sections obtained for the $^{90}\text{Zr}(n,p)^{90m}\text{Y}$ reaction include the contribution of the $^{91}\text{Zr}(n,d^*)^{90m}\text{Y}$ and $^{92}\text{Zr}(n,t)^{90m}\text{Y}$ reactions, and the contribution of the $^{92}\text{Zr}(n,t)^{90m}\text{Y}$ reaction can be neglected because its cross section is small (μb). The cross section values obtained for the $^{92}\text{Zr}(n,p)^{92}\text{Y}$ reaction include the contribution of the $^{94}\text{Zr}(n,t)^{92}\text{Y}$ reaction, which can be neglected because it has a very small cross section (μb). The cross sections obtained for the $^{94}\text{Zr}(n,p)^{94}\text{Y}$ reaction include the contribution of the

$^{96}\text{Zr}(n,t)^{94}\text{Y}$ reaction, which can be neglected, as it has a very small cross section (μb).

4 Results and discussion

In our work, the errors stem mainly from the counting statistics (0.2%-5.7%), standard cross section (1.1%-1.5%), detector efficiency (2.0%), sample weight (0.1%), sample geometry (1.0%), γ -ray self-absorption (1.0%-1.5%), and the fluctuation of the neutron flux (1.0%), among others.

For the $^{94}\text{Zr}(n,d^*)^{93\text{m}+g}\text{Y}$ reaction, as shown in Table 2 and Fig. 2, the trend of the theoretical excitation curve obtained by the computer code system Talys-1.9 increases with increasing incident neutron energy around 14 MeV. In the neutron energy range of 13.5-14.8 MeV, the fitted line of our experimental values is in good agreement with the theoretical excitation curve obtained by Talys-1.9. These two existing experimental datasets [2, 3] are well distributed on both sides of the theoretical curve, although there is a significant difference between them, which is reliable. The theoretical excitation curve generally matches these experimental data (including our results) reasonably well.

For the $^{96}\text{Zr}(n,\gamma)^{97}\text{Zr}$ reaction, Table 2 and Fig. 3 show that the fitting line of our results in the neutron energy range of 13.5-14.8 MeV is consistent with the theoretical excitation curve obtained by Talys-1.9 within the experimental error. The result of Pepelnik *et al.* [4] is considerably lower than that of the fitting line of our experimental values and that of the theoretical excitation curve obtained by Talys-1.9 at the corresponding energy, which is dubious. The result of Perkin *et al.* [6] is significantly higher than that of the fitting line of our experimental values and that of theoretical excitation curve obtained by Talys-1.9 at the corresponding energy, which is likewise dubious. The result of Wagner and Warhanek [5] is close to that of the fitting line of our experimental values and that of theoretical excitation curve obtained by Talys-1.9 at the corresponding energy.

For the $^{96}\text{Zr}(n,2n)^{95}\text{Zr}$ reaction, shown in Table 2 and Fig. 4, our experimental cross sections around the neutron energy of 14 MeV are in agreement, within the experimental error, with those of the fitting lines of Filatenkov [13], Molla *et al.* [15], and Hanlin Lu *et al.* [16] at the same energies as well as the theoretical values of the excitation curve obtained by Talys-1.9 at the corresponding energies. The three experimental datasets of Hanlin Lu *et al.* [16] at neutron energies of 16.86, 17.63, and 17.69 MeV are significantly lower than the theoretical excitation curves obtained by Talys-1.9 at the corresponding energies, which is dubious. The fitted line of our cross sections around the neutron energy of 14 MeV is consistent

with the theoretical excitation curve obtained by Talys-1.9 within experimental error.

The cross sections of the $^{90}\text{Zr}(n,\alpha)^{87\text{m}}\text{Sr}$ reaction are shown in Table 2 and Fig. 5. They show that the fitted line of our experimental cross sections is in agreement, within the experimental error, with the fitted line of the cross sections of Marcinkowski *et al.* [20], except for the two values at the neutron energies of 15.9 and 16.6 MeV as well as the theoretical excitation curve obtained by Talys-1.9. In contrast, the results of Filatenkov [13] and Semkova *et al.* [17] are overall higher. The results of Molla *et al.* [15] at neutron energies of 13.64 and 13.88 MeV are low, and at the neutron energies of 14.1, 14.58, 14.83 MeV, they are high.

For the $^{94}\text{Zr}(n,\alpha)^{91}\text{Sr}$ reaction, shown in Table 2 and Fig. 6, the fitted line of our experimental cross sections in the neutron energy range of 13.5-14.8 MeV is in agreement, within the experimental error, with the fitted line of the cross sections of Filatenkov [13] except for the three values at the neutron energies of 13.56, 13.74, and 13.96 MeV and the fitted line of Marcinkowski *et al.* [20], as well as the theoretical excitation curve obtained by Talys-1.9. In contrast, the results of Molla *et al.* [15] and the values of Filatenkov [13] at the neutron energies of 13.56, 13.74, 13.96 MeV are higher.

For the $^{90}\text{Zr}(n,p)^{90\text{m}}\text{Y}$ reaction, shown in Table 2 and Fig. 7, the results of Filatenkov [13], Molla *et al.* [15], Grallert *et al.* [19], Thiep *et al.* [22] are higher. In particular, the result of Sarkar and Bhoraskar [23] is significantly higher than all the other results, which is dubious. In contrast, the result of Osman and Habbani [18] is significantly lower than all the other results, which is also dubious. Our experimental cross sections are in agreement, within the experimental error, with those of the fitted line of the cross sections of Marcinkowski *et al.* [20] at the corresponding energies, as well as the theoretical values of the excitation curve obtained by Talys-1.9 at the corresponding energies.

For the $^{92}\text{Zr}(n,p)^{92}\text{Y}$ reaction, shown in Table 2 and Fig. 8, the fitted line of our experimental cross sections in the neutron energy range of 13.5-14.8 MeV is in agreement, within the experimental error, with the fitted lines of the cross sections of Filatenkov [13], Molla *et al.* [15] and Marcinkowski *et al.* [20]. The theoretical excitation curve obtained by Talys-1.9 generally matches these experimental data well.

For the $^{94}\text{Zr}(n,p)^{94}\text{Y}$ reaction, shown in Table 2 and Fig. 9, our experimental cross sections in the neutron energy range of 13.5-14.8 MeV are in agreement, within the experimental error, with those of the fitted line of the cross sections of Marcinkowski *et al.* [20] at corresponding energies. At the neutron energies of 13.5 and 14.1 MeV, our experimental values are in agreement, within the experimental error, with those of theoretical excita-

tion curve obtained by Talys-1.9 at the corresponding energies. The cross sections of Molla *et al.* [15] and Begun *et al.* [24] are higher than that of the fitted line of our experimental values and that of theoretical excitation curve obtained by Talys-1.9 at the corresponding energy. The theoretical excitation curve matches these experimental data well in general.

5 Conclusion

The experimental cross sections of the $^{94}\text{Zr}(n,d^*)^{93\text{m}+g}\text{Y}$, $^{96}\text{Zr}(n,\gamma)^{97}\text{Zr}$, $^{96}\text{Zr}(n,2n)^{95}\text{Zr}$, $^{90}\text{Zr}(n,\alpha)^{87\text{m}}\text{Sr}$, $^{94}\text{Zr}(n,\alpha)^{91}\text{Sr}$, $^{90}\text{Zr}(n,p)^{90\text{m}}\text{Y}$, $^{92}\text{Zr}(n,p)^{92}\text{Y}$, and $^{94}\text{Zr}(n,p)^{94}\text{Y}$ reactions have been measured in the neutron energy range of 13.5-14.8 MeV via the activation technique. The excitation curves of the above-men-

tioned eight nuclear reactions within the incident neutron energy range from the threshold to 20 MeV were obtained by adopting the nuclear theoretical model program system Talys-1.9. Generally, our experimental results agree with some previous experimental values, as well as those of the theoretical excitation curve obtained by Talys-1.9 at the corresponding energies. The theoretical excitation curves match the experimental data well.

The results obtained in the present work are useful for strengthening the database, and the theoretical excitation curves are significant for the development and utilization of nuclear energy and the related applications.

We thank the crew of the K-400 Neutron Generator at Institute of Nuclear Physics and Chemistry China Academy of Engineering Physics for performing the irradiation experiments.

References

- Experimental Nuclear Reaction Data (EXFOR) library, database version of May 31, 2020, International Atomic Energy Agency Nuclear Data Services. <<https://www-nds.iaea.org/exfor/>>
- S. M. Qaim, R. Woelfle, and G. Stoecklin, Rept: Euratom Reports, No.5182E(1974), Italy
- C. H. Reed, Rept: Div. of Tech. Info. U.S. AEC Reports, No.11929 (1960), USA
- R. Pepelnik, B. Anders, B. M.Bahal *et al.*, Rept: Ges. Kernen. Verwertung, Schiffbau and Schiffahrt, No.86-E-29 (1986), Germany
- M. Wagner and H. Warhanek, Acta Phys. Austriaca, **52**: 23 (1980)
- J. L. Perkin, L. P. O'Connor, and R. F. Coleman, Proc.Phys. Soc. London, **72**: 505 (1958)
- A. Koning, S. Hilaire, and S. Goriely, User Manual of Talys-1.9, 2017, <http://www.talys.eu/download-talys/>
- V. E. Lewis and K. J. Zieba, Nucl. Instrum. Methods, **174**: 141 (1980)
- NuDat-2 (selected evaluated nuclear structure data), IAEA Nuclear Data Services. <<https://www-nds.iaea.org/>>
- R. B. Firestone and V. S. Shirley, Table of Isotopes. Wiley, New York (1996)
- Xiangzhong Kong, Rong Wang, Yongchang Wang *et al.*, Appl. Radiat. Isot., **50**: 361 (1999)
- M. Wagner, H. Vonach, A. Pavlik *et al.*, Daten Phys. Data, **13-5**: 183 (1999)
- A. A.Filatenkov, Rept: USSR report to the I.N.D.C., No.0460 (2016), Austria
- Zhongsheng Pu, Xuebin Zhu, and Xiangzhong Kong, J. Lanzhou Univ., **39**: 107 (2003)
- N. I. Molla, R. U. Miah, M. Rahman *et al.*, Conf: Conf.on Nucl.Data for Sci.and Technol., 355 (1991), Germany
- Hanlin Lu, Wenrong Zhao, and Weixiang Yu, Chinese J. Nucl. Phys., **13**: 11 (1991)
- V. Semkova, E. Bauge, A. J. M.Plompen *et al.*, Nucl. Phys. A, **832**: 149 (2010)
- K. T. Osman and F. I. Habbani, Rept: Sudanese report to the I.N.D.C., No.001 (1996), Austria
- A. Grallert, J. Csikai, Cs. M.Buczko *et al.*, Rept: IAEA Nucl.Data Section report to the I.N.D.C., No.286(1993), Austria
- A. Marcinkowski, U. Garuska, H. M. Hoang *et al.*, Nucl. Phys.A, **510**: 93 (1990)
- K. Sailer, S. Daroczy, P. Raics *et al.*, Conf: 4.All Union Conf.on Neutron Phys., 1: 246 (1977), USSR246 (1977), USSR
- T. D. Thiep, N. V. Do, T. T. An *et al.*, Nucl. Phys.A, **722**: 568 (2003)
- R. Sarkar and V. N. Bhoraskar, Nucl. Phys.A, **633**: 640 (1998)
- S. V. Begun, N. R. Dzysiuk, I. M. Kadenko *et al.*, Yaderna Fizika ta Energetika, **8**: 42 (2007)
- Qiang Wang, Bingjun Chen, Qian Zhang *et al.*, Nucl. Sci. Tech., **30**: 8 (2019)
- Han Xue, Yugang Ma, Hongwei Wang *et al.*, Nucl. Tech., **41**: 110503 (2018)
- Fengqun Zhou, Yueli Song, Yong Li *et al.*, Chin. Phys. C, **43**: 094001 (2019)
- R. Baldik and A. Yilmaz, Nucl. Sci. Tech., **29**: 156 (2018)